

# Lawrence Berkeley National Laboratory

## Lawrence Berkeley National Laboratory

### **Title**

CRITICAL FIELD FOR SUPERCONDUCTIVITY AND LOW-TEMPERATURE NORMAL-STATE HEAT CAPACITY OF TUNGSTEN

### **Permalink**

<https://escholarship.org/uc/item/82k0f0j7>

### **Author**

Triplett, B.B.

### **Publication Date**

2008-12-01

CRITICAL FIELD FOR SUPERCONDUCTIVITY AND  
LOW-TEMPERATURE NORMAL-STATE  
HEAT CAPACITY OF TUNGSTEN

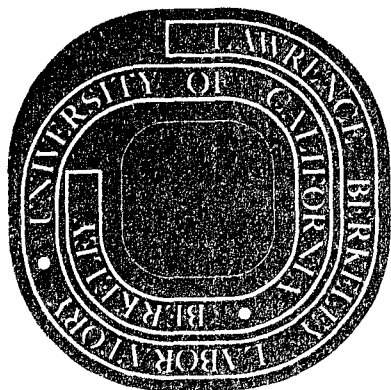
B. B. Triplett, N. E. Phillips, T. L. Thorp,  
D. A. Shirley, and W. D. Brewer

March 1973

Prepared for the U. S. Atomic Energy  
Commission under Contract W-7405-ENG-48

TWO-WEEK LOAN COPY

*This is a Library Circulating Copy  
which may be borrowed for two weeks.  
For a personal retention copy, call  
Tech. Info. Division, Ext. 5545*



LBL-1497  
*c.j.*

Critical Field for Superconductivity and Low-Temperature  
Normal-State Heat Capacity of Tungsten\*

B. B. Triplett,<sup>†</sup> N. E. Phillips, T. L. Thorp<sup>‡</sup>,  
D. A. Shirley, and W. D. Brewer<sup>‡</sup>

Lawrence Berkeley Laboratory  
and Department of Chemistry,  
University of California  
Berkeley, California 94720

ABSTRACT

We have measured the critical magnetic field for superconductivity in tungsten from 5.5 to 15 mK using a  $\gamma$ -ray anisotropy thermometer, and we have measured the heat capacity between 0.35 and 25 K. Analysis of the data gives  $H_0 = 1.237$  Oe for the 0 K critical field,  $T_C = 16.0$  mK for the critical temperature,  $\gamma = 1.008$  mJ/mole K<sup>2</sup> for the coefficient of the electronic heat capacity, and  $\Theta_0 = 383$  K for the 0 K Debye temperature. The measured values of the critical field  $H_C$  are consistently higher than those reported by Black, Johnson and Wheatley (BJW) on the CMN temperature scale, but the temperature dependence is similar. This discrepancy and the temperature dependence of  $H_C$  suggest that both sets of  $H_C$  data are affected by magnetic impurities. Use of the calorimetric  $\gamma$  value permits an improved test of the CMN temperature scale with the very low temperature  $H_C$  data obtained by BJW.

## I. INTRODUCTION

Superconductivity in tungsten was discovered by Gibson and Hein.<sup>1</sup> Experimental problems prevented an accurate determination of the critical temperature  $T_C$  but, by comparison with the magnetic susceptibility of chromium potassium alum, they estimated upper and lower limits of 11 and 5 mK. Johnson et al.<sup>2</sup> confirmed the existence of a superconductivity transition at  $T_C \approx 12$  mK and measured the critical field  $H_C$ . Their measurements were referred to the magnetic temperature scale  $T^*$  (proportional to the reciprocal of the magnetic susceptibility) for a right circular cylinder with height equal to diameter of CMN [ $\text{Ce}_2\text{Mg}_3(\text{NO}_3)_{12} \cdot 24 \text{H}_2\text{O}$ ]. A third, more extensive series of measurements of the temperature dependence of  $H_C$  has been described by Black<sup>3</sup> and by Black, Johnson and Wheatley,<sup>4</sup> hereafter referred to as BJW. They used the same CMN temperature scale, but improved the thermal contact between the tungsten sample and the CMN, and found  $T_C = 15.4$  mK.

The CMN temperature scale (we use this term to designate the magnetic temperature measured with powdered CMN and the geometry described above) is of considerable interest because it is the basis for a number of measurements<sup>5</sup> of the properties of liquid  $^3\text{He}$  and dilute solutions of  $^3\text{He}$  in  $^4\text{He}$ . The observed temperature dependence of  $H_C$  for tungsten has been discussed<sup>3,4</sup> as a test of the accuracy with which this scale reproduces the thermodynamic temperature scale. The test is based on the thermodynamic relation

$$dH_C^2/dT^2 = -(4\pi/VT)[S_N(T) - S_S(T)] \quad (1)$$

where  $S_S$  and  $S_N$  are the superconducting- and normal-state molar entropies and  $V$  is the molar volume, and on the BCS expression<sup>6</sup> for  $H_C(T)$ . Eq.(1) was used in the low-temperature limit in which  $S_N(T) - S_S(T) \sim T$ , where  $\gamma$  is the coefficient of the electronic heat capacity. With that approximation (neglect of all contributions to  $S_S - S_N$  except the normal-state electronic entropy) Eq.(1) can be integrated to give

$$H_C^2 = H_0^2 - (4\pi\gamma/V) T^2 . \quad (2)$$

Possible discrepancies between  $T^*$  and  $T$  are usually represented by

$$\Delta \equiv T - T^* . \quad (3)$$

With  $\Delta = 0$ , BJW found a linear relation between  $H_C^2$  and  $T^2$  for  $3 \leq T \leq 4.5$  mK. The slope of  $H_C^2$  vs.  $T^2$  corresponded to  $\gamma = 0.90$  mJ/mole  $K^2$ , in reasonable agreement with some recent heat capacity measurements<sup>7,8</sup> which give  $\gamma$  values of 0.84 and 0.95 mJ/mole  $K^2$ . Above 4.5 mK where, according to the BCS theory, Eq.(2) is not accurate, BJW analysed their data using different constant values of  $\Delta$ . The choice  $\Delta = 0 \pm 0.2$  mK gave significantly better fits to the BCS theory than did other constant values of  $\Delta$ . It was concluded<sup>3,4</sup> that large values of  $\Delta$  (of the order of 1 mK) which have been suggested by other work<sup>9</sup> were inconsistent with the  $H_C$  measurements and that for  $T \gtrsim 3$  mK,  $\Delta \approx -0.01$  mK if the criterion of best fit to the BCS theory is accepted. At temperatures below 3 mK, deviations from a linear dependence of  $H_C^2$  on  $T^{*2}$  were observed and were attributed to discrepancies between  $T^*$  and  $T$ .

The tungsten critical field measurements reported here were originally undertaken to test apparatus that was used for a search<sup>10</sup> for superconductivity in lithium and magnesium.  $H_c$  was measured as a function of the temperature indicated by  $\gamma$ -ray anisotropy thermometers. The importance of the value of  $\gamma$  as a test of the thermodynamic consistency of the  $H_c$  data and the discrepancies between previously reported  $\gamma$  values suggested that a new heat capacity measurement would be useful. The heat capacity was therefore measured between 0.35 and 25 K. The results give a new set of values for the parameters characterising the lattice and electronic heat capacities and the superconducting transition in tungsten. Furthermore, comparison with the earlier  $H_c$  measurements<sup>3,4</sup> gives an indirect but still interesting comparison of the CMN and  $\gamma$ -ray anisotropy temperature scales.

## II. SAMPLES

The tungsten samples used in this work and by BJW were all purchased from Semi-Elements Inc.<sup>11</sup> They all had the same nominal purity, 99.999%, but the residual resistivities of the various samples differed considerably. Table I shows the measured resistivity ratios as well as ratios corrected for the effects of current and size dependence. Since the samples used in this work were polycrystalline and had higher resistance ratios than the single crystal used by BJW, they can be assumed to have lower levels of impurities.

### III. HEAT CAPACITY MEASUREMENTS

#### A. Apparatus and Experimental Techniques

The tungsten sample used in the heat capacity measurements weighed 80 g. It was attached to the mounting thread at the bottom of the sample holder-thermometer-heater assembly shown in Fig. 1 by a threaded copper bushing. The sample itself was not threaded but was slightly tapered on the mounting end and jammed into the bushing. The differential thermal contraction produced good thermal contact. (No thermal bonding agent was necessary, and none was used.) Thermal equilibrium in the sample-sample holder system was always attained more rapidly than the time constant of the measuring instruments, approximately 0.3 sec. The thermometer was not superheated perceptibly above the final sample temperature with any heater power used in the measurements. The heat capacities of the sample holder and copper bushing were determined in separate experiments.

Thermal contact between the sample holder and the  $^3\text{He}$  pot of a  $^3\text{He}$  evaporation refrigerator was made by a mechanical heat switch. The jaws of the switch were attached to the pot by flexible copper wires and closed on the heat switch wire of the sample holder. The pot could be regulated at any temperature between 0.3 K and 25 K. At temperatures below 1 K the heat of vaporization of the  $^3\text{He}$  was balanced by the heat leak from the  $^4\text{He}$  bath at 1 K and an automatically regulated electrical heat input. At temperatures above 1 K the electrical heat input balanced the heat leaking out to the bath. No exchange gas was used in cooling the sample below 77 K, and no He exchange gas was used at any time.

A superconducting solenoid (not shown in Fig. 1) was located in the <sup>4</sup>He bath and could produce fields up to 38 kOe on the sample. The stray magnetic field on the germanium thermometer with 38 kOe at the sample was reduced to approximately 1 Oe by a mumetal shield surrounding the thermometer (also not shown in Fig. 1). Without this shield the stray field would have been approximately 100 Oe.

The germanium resistance thermometer was calibrated in a different cryostat that was designed for the purpose. The calibration was based on  $T_{58}$ , the 1958 <sup>4</sup>He vapor pressure scale,<sup>13</sup> between 1.2 and 4.2 K and the magnetic temperature of a spherical single crystal of CMN below 12. K. Above 4.2 K, the thermometer was compared with a constant-volume gas thermometer, which was referred (at 20 K) to a platinum thermometer calibrated on the NBS (1955) scale.<sup>14</sup> The gas thermometer gave temperatures 4 mK lower than  $T_{58}$  at 4.2 K, but the discrepancy was within the uncertainty associated with the virial coefficient corrections. (To obtain good precision, a rather high filling pressure had been used.) The heat capacity data are reported on a scale that agrees with  $T_{58}$  at 4.2 K and with the NBS (1955) scale at 14 K. In the intervening region the scale was interpolated using both the gas thermometer data and a thermometer calibrated on the NBS acoustic scale<sup>15</sup> (which is 10 mK higher than  $T_{58}$  at 4.2 K) as guides.

The heat capacities of various copper samples have been measured with the same sample holder-thermometer-heater assembly<sup>16</sup> and the results are generally in good agreement with other recent measurements.<sup>17,18</sup> For pure copper  $\gamma$  was estimated to be 0.693 mJ/mole K<sup>2</sup>. (For the purest



sample actually studied, which contained approximately 2 at ppm of iron,  $\gamma$  was 0.695 mJ/mole K<sup>2</sup>.) Between 1 and 22 K, the total heat capacity of copper determined in these measurements agreed to within 0.5% with the reference equation<sup>17</sup> found to represent several other independent measurements. That equation is also in good agreement with two more recent sets of data that were not considered in its derivation.<sup>19,20</sup>

#### B. Results and Comparison with Other Measurements

The heat capacity was measured in zero magnetic field and in 38 kOe. The high field measurements were made to test for a possible contribution to the heat capacity associated with magnetic impurities. As shown in Figs. 2 and 3, any difference between the zero-field and 38 kOe heat capacities is not large compared with the scatter of the data. This shows that the heat capacity is not affected by magnetic impurities that have Kondo temperatures or spin-spin ordering temperatures of the order of a few K or lower. For impurities for which these characteristic temperatures are high, the heat capacity contribution per impurity is small at low temperatures. A significant contribution to the heat capacity by impurities of this type is precluded by the known low total impurity concentration.

With the usual assumptions, the low-temperature heat capacity of a normal metal is the sum of the electronic heat capacity,  $C_E = \gamma T$ , and the lattice heat capacity,  $C_L = A_3 T^3 + A_5 T^5 + \dots$ . Therefore,

$$C = C_E + C_L = \gamma T + A_3 T^3 + A_5 T^5 + \dots, \quad (4)$$

and the separation of  $C_E$  and  $C_L$  depends on fitting the data with Eq.(4). Both graphical methods, illustrated in Figs. 2 and 3, and least-squares methods of analysis have been used. The values obtained for the various parameters in Eq.(4) depend on the temperature interval included in the analysis and their accuracy appears to be limited by temperature scale errors. Least squares fits of the data to a number of expressions of the form of Eq.(4) have shown that the omission of the  $T^5$  term does not significantly reduce the rms deviation. The data can be fitted with an rms deviation of 0.51% with only the  $T$ ,  $T^3$ , and  $T^7$  terms. The deviations are systematic and, at some temperatures, up to 1% magnitude, as illustrated in Fig. 3. However, they are similar in temperature dependence and magnitude to the deviations of the heat capacity of copper from an expression that included  $T$ ,  $T^3$ ,  $T^5$ , and  $T^7$  terms. For this reason we believe that the deviations of  $C$  from the three-term fit are largely a reflection of errors in the temperature scale, and that the best estimate of  $A_7$  is obtained from a fit of this type or from a graphical analysis of the type illustrated in Fig. 3. The rms deviation is reduced to 0.45% by inclusion of  $T^9$  and  $T^{11}$  terms, and the deviations are more nearly random, but the corresponding values of  $A_7$ ,  $A_9$ , and  $A_{11}$  probably have no relation to the properties of tungsten. The coefficients determined by these fits are given in Table II. For the last fit given in Table II, only eleven points, nine of them below 1 K, deviate from the equation by 0.5% or more. The values of  $\gamma$  obtained by various least-squares fits to Eq.(4) are very similar to the value, 1.008 mJ/mole  $K^2$ , given by the graphical analysis of the below-4 K data shown in Fig. 2. The values of  $A_3$  given by the least-squares fits and

by the graphical analysis in Fig. 2 are all higher than that given by the graphical analysis of Fig. 3, in which more weight is given to higher temperature data. This discrepancy is apparently associated with an inconsistency between  $T_{58}$  and the scale used at higher temperatures. Suggested values of the various parameters are:  $\gamma = 1.008 \pm 0.010$  mJ/mole  $K^2$  (from Fig. 2);  $A_3 = 0.0346 \pm 0.0006$  mJ/mole  $K^4$  (an average of values from Figs. 2 and 3 and from least-squares fits);  $A_5 = 0 \pm 2 \times 10^{-6}$  mJ/mole  $K^6$  (from plots of  $C_L/T^3$  vs.  $T^2$  and least-squares fits);  $A_7 = 2.8 \pm 0.5 \times 10^{-8}$  mJ/mole  $K^8$  (from Fig. 3). The indicated uncertainties are essentially guesses as to the possible magnitudes of systematic errors, but they are intended to be generous. The value of  $A_3$  corresponds to a 0 K Debye characteristic temperature  $\theta_0 = 383.0 \pm 2.2$  K.

Several other measurements of the low temperature heat capacity of tungsten have been reported recently. Maita<sup>7</sup> found  $\gamma = 0.84$  mJ/mole  $K^2$  and Bucher, Heiniger and Muller<sup>8</sup> report  $\gamma = 0.95 \pm 0.05$  and  $\theta_0 = 396 \pm 10$ . Our measurements are in reasonable agreement with the latter, in view of the estimated uncertainties, but there appears to be a substantial disagreement with the former (the data have not been reported in detail so there is no basis for estimating the probable error). Our measurements are also in good agreement with measurements between 4 and 15 K by Waite, Craig and Wallace<sup>21</sup> who found  $\gamma = 1.1 \pm 0.1$  and  $\theta_0 = 378 \pm 7$  K. Ordinarily, measurements in that temperature range would not give reliable values of  $\gamma$  or  $\theta_0$ . However, for tungsten  $\theta_0$  is relatively high (the electronic heat capacity is 60% of the total at 4 K) and the  $T^3$  approximation for the lattice heat capacity is

valid to above 10 K. For these reasons it is quite possible to obtain accurate values of  $\gamma$  and  $\theta_0$  from measurements above 4 K.

#### IV. CRITICAL FIELD MEASUREMENTS

##### A. Apparatus and Experimental Techniques

The tungsten sample used in the critical field measurements was a 1/8 in. diameter rod 1.3 in. long. The sample was placed in thermal contact with a slurry of powdered CMN through a bundle of approximately 5000 #40 AWG Heavy Formex insulated copper wires that were potted in Epibond 100 A to form a rigid stalk. Contact between the stalk and the sample was made by grinding the end of the stalk to form a large flat area at a sharp angle to its axis. One end of a strip of copper foil that was divided into narrower strips at both ends was tied to the flat on the stalk with fine copper wires and a heavy copper layer was electroplated over the narrow strips and the intervening exposed areas of the flat. The other end of the strip was attached in a similar way to a gold layer bonded to the tungsten sample. The gold layer was produced by evaporating a layer of gold 0.4 in. long at one end of the sample and partially diffusing the gold into the tungsten by heating at 1200°C for approximately 1/2 hr. It is estimated that the gold penetrated to a depth of the order of 0.1 mm.

Temperatures were measured with a single crystal  $^{60}\text{Co}$  Co nuclear orientation thermometer that was attached by electroplating to a lower flat on the stalk. The sample was cooled by simultaneous demagnetization

of the CMN and a chromium potassium alum guard salt from 46 kOe and 1 K. The magnetizing field was produced by a superconducting solenoid in the 1 K bath that was raised above the liquid helium after completion of the demagnetization. The solenoid became normal within approximately 15 min of the time it was raised, and was also a considerable distance from the sample after this operation. No other materials that would have become superconducting at their working temperatures were used in the apparatus. The superconducting-normal transition was detected by mutual inductance coils coupled to the sample. A 17 Hz, 3 mOe rms primary field was used and the detection system gave a signal to noise ratio of 50 (time constant 3 sec). The transitions were observed at approximately constant temperature by sweeping an axial DC field produced by a separate winding on the mutual inductance coil assembly. Low noise current for the winding was provided by a voltage programmable current supply. The experimental arrangement is described in more detail in Reference 10.

Several indications of the adequacy of the thermal contact between the sample and thermometer were obtained. The most direct is that increasing the primary field to 21 mOe rms had no observable effect on the measured critical fields even though it doubled the upward temperature drift of the thermometer-sample assembly. The rate at which the transitions occurred also demonstrates good thermal contact to the sample. The transitions required a maximum of 5 sec to go to completion. This behavior can be contrasted with that in the experiment by BJW in which the rate of the transition was limited by the Kapitza<sup>2</sup> resistance between the sample and the surrounding <sup>3</sup>He bath, and the time required

for the transition was several minutes. The self heating in the  $\gamma$ -ray thermometer was approximately 4 erg/min. For experiments limited by a Kapitza resistance between sample and thermometer this would be a relatively high power level, but it should produce a temperature difference across a clean metallic contact of no more than  $10^{-4}$  mK. Although no direct measure of the thermal resistance between the thermometer and the stalk was obtained in this particular experiment, our experience shows that  $\gamma$ -ray thermometers mounted in the same way but with twenty times the self heating indicated the same temperature.

Stray fields at the sample were compensated with three pairs of Helmholtz coils. In the absence of the sample but with the apparatus at actual operating temperatures, flux-gate magnetometer and rotating coil gaussmeter probes could be placed at the sample position in a moveable superinsulated hot finger. The field was adjusted to  $0 \pm 2$  mOe and the field gradients to  $0 \pm 1$  mOe/cm. During critical field measurements the probe was placed 2 in. above the sample and used to monitor changes in field. It had been hoped that the stray field would be sufficiently constant that it could be nulled by constant currents in the Helmholtz coils that were adjusted before an experiment. However, an unforeseen problem interfered -- operation of the 46 kOe solenoid changed the laboratory stray field. Immediately after demagnetization the axial field at the sample site was 35 mOe greater than it had been before the solenoid was turned on. The stray field decayed to 2 mOe during the period required for a series of measurements, but the decay

was not precisely regular. During the measurements the axial field 2 in. above the sample was compared at intervals with the value deduced by measuring the critical field with opposite polarities of the applied field. The accuracy of the latter method of determining the stray axial field was limited primarily by the temperature drift between measurements. The two methods of measuring the axial stray field differed by as much as 20%, even when it was greater than 10 mOe. In correcting for the stray axial field greater weight was given to the values estimated by observing the transition with applied fields of opposite polarities, but values measured with the probe were used for interpolating in time. The uncompensated stray field after a demagnetization also had a horizontal component but it was considerably smaller -- a maximum of 7 mOe. It was not possible to monitor this component during the measurements and no correction has been made for it. The estimated overall accuracy of the critical field measurements is 10 mOe at the lowest temperatures and 2 mOe near  $T_c$ .

An additional complication in the critical field measurements was the appearance at the lowest temperatures of a second transition. It occurred at lower critical fields and produced a change in mutual inductance about 1/3 as great as that associated with the main transition. We have been unable to devise a completely satisfactory explanation for the occurrence of the second transition, but we suspect it was associated with the end of the sample to which the gold diffusion bond was made and which was just outside the secondary coils. Both transitions were very sharp and apparently completely independent. The second

transition, when it occurred, seemed to have no effect on the main transition. The data reported here were obtained in a single run that extended to 5.2 mK. The points taken below 5.5 mK were complicated by superheating effects as well as by the second transition and have been omitted.

### B. Results and Comparison with Other Measurements

The results of the critical field measurements are shown in Fig. 4 as  $H_C$  vs.  $T^2$ , and the data below 9 mK are also shown as  $H_C^2$  vs.  $T^2$  in Fig. 5. We have used two different procedures to extrapolate  $H_C$  to 0 K to obtain  $H_0$ . The first method was based on the BCS expression for  $H_C$ , and the second on Eq.(2).

Tungsten certainly corresponds to the weak-coupling limit treated in the BCS theory, and the deviations of the  $H_C$  data from a parabolic temperature dependence,  $H_C = H_0 [1 - (T/T_C)^2]$ , are in qualitative agreement with those predicted by the BCS theory (see Fig. 4). It therefore seems reasonable to base the extrapolation of  $H_C$  to 0 K on the BCS expression. As shown in Figs. 4, 5 and 6a, the  $H_C$  data do fit the BCS theory to within the precision of the measurements. The quantity plotted in Fig. 6 is the deviation,  $D(t) \equiv h - (1 - t^2)$ , of the reduced critical field,  $h \equiv H_C/H_0$ , from a parabolic dependence on reduced temperature,  $t \equiv T/T_C$ . The value of  $T_C$  was found by the procedure used by BJW: an approximate value for  $H_0$  and a high temperature expansion<sup>22</sup> based on BCS theory for  $H_C(T)$  were used to find a preliminary value of  $T_C$ . That value of  $T_C$  and numerical tables<sup>23</sup> of the BCS



functions were then used to adjust  $H_0$  to give better agreement with the theoretical  $D(t)$  at low temperatures. Finally, the new  $H_0$  value was used to recalculate  $T_c$ . The numerical values are  $H_0 = 1.224$  Oe, and  $T_c = 15.98$  mK.

Although the critical field data can be fitted with the BCS theory, an inconsistency becomes apparent when the calorimetric data are included in the comparison. The  $\gamma$  value that corresponds to the representation of the critical field data by BCS theory is given by

$$\frac{2\pi\gamma T_c^2}{VH_0^2} = 1.057, \quad (5)$$

and is  $\gamma = 0.94$  mJ/mole  $K^2$ . (We have used  $V = 9.508$  cm<sup>3</sup>/mole, as calculated from the lattice parameter<sup>24</sup> and thermal expansion.<sup>25</sup>) This value differs significantly from that determined calorimetrically. The calorimetric value requires larger (negative) slopes of  $D(t)$  vs.  $t^2$  and  $H_c^2$  vs.  $T^2$  in the 0 K limit. For example, Eq.(2) requires that  $[dD(t)/dt^2]_{t=0} = -[(2\pi\gamma T_c^2/VH_0^2)-1]$ ; the calorimetric  $\gamma$  value gives an initial slope  $-0.113$ , whereas the BCS theory gives  $-0.057$ .

The BCS expression for  $H_c$  and Eq.(2) agree to within 0.2% for  $t \leq 0.3$  (but diverge rapidly at higher temperatures). If  $H_c^2$  is extrapolated to 0 K from our lowest-temperature data with the slope required by Eq.(2) and  $\gamma = 1.008$  mJ/mole  $K^2$ , the value of  $H_0$  is increased to 1.237 Oe. The values of  $D(t)$  are then considerably more negative than predicted by the BCS theory. This interpretation of the

critical field data is also represented in Figs. 5 and 6b. It corresponds to a superconducting-state entropy that increases more rapidly with increasing temperature than BCS theory predicts for the values of  $\gamma$  and  $T_c$ . If it is assumed that  $H_c^2$  follows the BCS curve in Fig. 5 to a lower temperature and the slope changes to the value required by Eq.(2) only at a temperature well below the lowest temperature critical field data, the affect on  $H_0$  and  $D(t)$  is smaller, but the implication for the temperature dependence of the superconducting-state entropy is similar. In fact, since  $H_c$  depends only on  $S_N-S_S$ , the BCS extrapolation of  $H_c^2$  to 0 K indicated in Fig. 5 would be consistent with the calorimetric  $\gamma$  value if there were a linear term in the superconducting-state entropy.

The critical field data reported by BJW are also represented in Figs. 4-6. (We have corrected their data, according to the formula they suggest, for the effect of the field produced by the CMN on the tungsten sample, and we have taken their reported values of  $H_0$  and  $T_c$  in which this correction is included.) Their  $H_c$  data are consistently lower than ours, and their values for  $H_0$  and  $T_c$ , 1.15 0e and 15.4 mK, are lower by 6% and 4% respectively. On the other hand, the relation between their data, BCS theory, and the calorimetric  $\gamma$  value is strikingly similar to that found in this work. BJW's data extend below 4.5 mK, the temperature at which BCS theory predicts that Eq.(2) becomes accurate to 0.2%. Between that temperature and 3 mK their data give a straight line when plotted as  $H_c^2$  vs.  $T^2$  but deviations occur below 3 mK. They attributed the deviations to a nonzero  $\Delta$  (Eq.(3)) below

3 mK and extrapolated the straight line to 0 K to obtain  $H_0$ .  $T_c$  was obtained by the extrapolation procedure based on BCS theory described above. As shown in Fig. 6a the values of  $D(t)$  found by BJW are similar to those found in this work by using BCS expressions to extrapolate to 0 K, and are in good agreement with BCS theory. However, the value of  $\gamma$  calculated from the  $H_c^2$  vs.  $T^2$  straight line and Eq.(2) is 0.90 mJ/mole K, also in disagreement with the calorimetric  $\gamma$  value.

## V. DISCUSSION

### A. Critical Field

Experimental errors -- either in the measurement of the critical field or in the temperature scales -- may contribute to the difference between our critical field measurements and those by BJW, but there is reason to think that a large part of the difference is a reflection of a real difference in the properties of the two samples. When analyzed in similar ways, both sets of data give similar values for  $D(t)$  and for  $\gamma$ . (The agreement between the  $\gamma$  values is not as good as might be expected from critical field measurements made under ideal conditions, but it is very good in view of the special experimental problems associated with the low value of  $T_c$ .) As described below, this can easily be understood as a consequence of different impurity levels in the samples, but an understanding on any other basis would require implausible experimental errors. Figure 4 shows that the required error is an approximately constant additive error in critical field or in the square of the temperature (or some equivalent combination of the two). In both

sets of measurements the stray axial field was checked by measuring critical fields with opposite polarities of the applied field and any undetected perpendicular field would add vectorially. The apparent difference in  $T_c$  values is not large compared with the combined estimated uncertainties in temperature at that temperature, but the discrepancy in temperature at the lowest temperatures is well outside reasonable error limits. Furthermore, it is difficult to see how a constant error in the square of the temperature, over the range of temperature involved, could occur in either measurement.

Concentrations of impurities too low to have a perceptible effect on equilibrium normal-state properties, in particular  $\gamma$ , can have a substantial effect on superconducting-state properties and, therefore, on parameters related to the transition. Experimental evidence suggests that low concentrations of nonmagnetic impurities generally lower  $T_c$ .<sup>26</sup> The effect is produced by a reduction in the energy of condensation to the superconducting state associated with the energy gap anisotropy in the clean sample and the reduction in electron mean free path.<sup>27,28</sup> At very low concentrations the reduction in  $T_c$  is proportional to the concentration of impurities, but there is a maximum to the reduction, observed for electron mean free paths short compared with the coherence distance.<sup>27,28</sup> If we assume a typical value for the energy gap anisotropy of tungsten, of the order of a few percent, it appears that this effect cannot account for the difference between our sample and that used by BJW.<sup>29</sup> Impurities with localized magnetic moments, however, can have a

greater effect on  $T_c$  through their reduction of the lifetime of the Cooper pairs, and they also affect the temperature dependence of the superconducting state entropy in the way suggested by our critical field measurements when they are analyzed in conformity with Eq.(2). Values of  $dT_c/dc$ , where  $c$  is the concentration of magnetic impurities, of the order of 1 to 10 mK/at ppm have been reported.<sup>30</sup> A magnetic impurity concentration of the order of 1 at ppm is not inconsistent with the heat capacity data, and seems entirely possible for both samples. Since both samples were obtained from the same supplier and that used by BJW had a higher residual resistivity, it is reasonable to consider that the difference in  $T_c$  is associated with a higher concentration of magnetic impurities in BJW's sample.

In the presence of magnetic impurities the superconducting-state entropy increases more rapidly as the temperature increases from zero, and  $D(t)$  is shifted to more negative values than given by BCS theory, particularly at low reduced temperatures. Decker and Finnemore<sup>31</sup> have calculated  $D(t)$  for various values of  $T_c/T_{cp}$ , where  $T_{cp}$  is the value of  $T_c$  in the absence of magnetic impurities, using an extension<sup>32</sup> of the Abrikosov-Gorkov<sup>33</sup> (AG) theory. The calculated  $D(t)$  curves are in good agreement with experiment for ThGd alloys.<sup>31</sup> For  $T_c/T_{cp} = 0.8$  and  $0.6$  they are reproduced in Fig. 6b and it is apparent that they are in qualitative agreement with the critical field data when those data are extrapolated to 0 K in accord with Eq.(2). [For  $T_c/T_{cp}$  in the region 0.6 to 0.8 the superconductor is gapless only near  $T_c$ ,  $S_s(T)$  varies exponentially with  $T$  for  $T \ll T_c$ , and Eq.(2) is still valid.<sup>32,33</sup>]

The presence of plausible concentrations of magnetic impurities would thus account in a straightforward way for a large part of the

discrepancy between our critical field measurements and those by BJW. It would also account for the discrepancy between the calorimetric  $\gamma$  value and the value obtained by an analysis of the critical field measurements based on BCS theory. Although not supported by conclusive evidence, such an interpretation is reasonable, and suggests that the superconducting-state properties of all samples of tungsten studied so far are significantly influenced by magnetic impurities. Detailed information on the impurities in our sample and in BJW's might permit an estimate of  $T_{cp}$  from the two observed values of  $T_c$ , but it is not available and would be extremely difficult to obtain for such low impurity concentrations. An approximate upper limit to  $T_{cp}$  is suggested by Fig. 6b, however. Recalling that the points in that figure represent a probable upper limit to  $|D(t)|$ , we can say that  $T_{cp}$  might be as high as 20 mK. The general shape of  $D(t)$  defined by the experimental points suggests that this value may be approximately correct, but the precision of the data do not permit a firm estimate.

#### B. Electronic Heat Capacity

The measured value of  $\gamma$  corresponds to a density of electronic states at the Fermi energy  $N(0) = 0.43$  states of both spins/eV atom. Band structure calculations give the "bare" or "band-structure" density of states  $N_{bs}(0) = N(0)/(1+\lambda)$  where  $\lambda$  is the electron-phonon interaction parameter. McMillan's<sup>34</sup> formula for  $T_c$  and his suggested approximate value of 0.13 for the coulomb repulsion term  $\mu^*$  permit an estimate of  $\lambda$

from the experimental  $T_c$  and  $\theta_0$ . The result is  $\lambda = 0.27$  which gives  $N_{bS}(0) = 0.34$  states of both spins/eV atom. Mattheiss<sup>35</sup> has calculated two values of  $N_{bS}(0)$ , 0.56 and 0.32 states of both spins/eV atom, using a nonrelativistic augmented-plane-wave (APW) method and two different potentials. Loucks has derived  $N_{bS}(0) = 0.640$  states of both spins/eV atom from a nonrelativistic APW calculation<sup>36</sup> and  $N_{bS}(0) = 0.368$  states of both spins/eV atom from a relativistic APW calculation.<sup>37</sup> The "experimental" value of  $N_{bS}(0)$  is sensitive to the value of  $\lambda$  and, therefore, to the assumed value of  $\mu^*$ . However, any error introduced into the experimental value by the assumed value of  $\mu^*$  is probably smaller than the error in the theoretical values that is apparently associated with uncertainty in the potential.

### C. Lattice Heat Capacity

The lattice heat capacity of tungsten is shown in Fig. 7 as a plot of the effective Debye temperature  $\theta$  as a function of temperature. ( $\theta$  is defined by equating the experimental heat capacity data to the Debye heat capacity function of  $\theta/T$ .) The values of  $\theta$  exhibit the usual decrease with increasing temperature. However, the curve is somewhat unusual in that  $\theta$  is constant up to  $\theta_0/T = 30$ , corresponding to the small value of  $A_5$ . The solid square in Fig. 7 represents the value of  $\theta_0$ , 384.3 K, calculated from sound velocity measurements.<sup>38</sup> It agrees with the calorimetric value, 383.0 K, to within the estimated uncertainties.

#### D. CMN Temperature Scale

If the above interpretation of the critical field data is accepted, the deviations from Eq.(2) of the low-temperature data obtained by BJW can be used as a test of possible  $T(T^*)$  relations for CMN. It is not practical to derive the correct  $T(T^*)$  relation from such data alone because several different  $T(T^*)$  relations may give satisfactory agreement with Eq.(2). This is illustrated in Fig. 8 where it is shown that  $\Delta = -0.4$  mK and  $T^2\Delta = 9$  mK<sup>3</sup> both give reasonable agreement between the data and Eq.(2). The latter relation is similar in temperature dependence to that obtained by Webb et al.<sup>39</sup> with a Johnson noise thermometer, but it gives considerably larger values of  $\Delta$  (eg., at  $T^* = 2.0$  mK,  $\Delta = 1.0$  mK, compared with  $\Delta = 0.4$  mK from the noise thermometer measurements). However, the test of the  $T(T^*)$  relation based on the critical field data is quite sensitive to the correction for the contribution to the field applied to the tungsten sample from the magnetic moment of the CMN. The  $T^2\Delta = 9$  mK<sup>3</sup> estimate was based on a correction proportional to  $1/T^*$  and equal to 2% at 1 mK, but the estimated uncertainty in the correction is  $\pm 50\%$ , and use of the largest correction within this range would reduce the value of  $T^2\Delta$  obtained from the critical field data (to give  $\Delta = 0.8$  mK at  $T^* = 2.0$  mK). Furthermore, it is clear that more complicated expressions for  $\Delta(T)$  could be found that would give reasonable consistency with Eq.(2) and also with the noise thermometer data. For example,  $T^2(\Delta+0.3) = 3$  mK<sup>3</sup> gives good agreement with Eq.(2) and also gives  $\Delta = 0.4$  mK at  $T^* = 2.0$  mK. However, this relation is certainly



not unique in these respects. On the other hand, the critical field data are clearly not consistent with a positive, temperature-independent  $\Delta$ . As previously noted by Black<sup>3</sup> such a value of  $\Delta$  increases the curvature of the low-temperature  $H_C^2$  vs.  $T^2$  plot, but it also tends to lower the value of  $\gamma$  deduced from the  $H_C$  data and therefore to increase the discrepancy with the calorimetric value.

## VI. SUMMARY

The heat capacity of tungsten has been measured between 0.35 and 25 K. The value of  $\gamma$ , 1.008 mJ/mole K<sup>2</sup>, is within the rather broad range of previously reported values and is believed to be accurate to 1%. The value of  $\theta_0$ , 383 K, is in good agreement with that calculated from elastic constants. In this temperature region the accuracy of the temperature scale limits the accuracy with which the various terms in the lattice heat capacity can be determined, but within this limitation the lattice heat capacity can be represented by a sum of  $T^3$  and  $T^7$  terms.

The critical field for superconductivity in tungsten has been measured between 5.5 and 15 mK using a  $\gamma$ -ray anisotropy thermometer. Analysis of the data gave  $H_0 = 1.237$  Oe and  $T_C = 16.0$  mK. The measured values of  $H_C$  are consistently higher than those reported by BJW. This discrepancy and discrepancies between the calorimetric  $\gamma$  value and the low-temperature slopes of  $H_C^2$  vs.  $T^2$  suggest that the superconducting-state properties of both samples are influenced by magnetic impurities.

The critical field data obtained by BJW below 4.5 mK on the powdered CMN  $T^*$  scale were reanalyzed using the calorimetric  $\gamma$  value. This analysis confirms that positive temperature independent values of  $\Delta = T - T^*$  are inconsistent with the critical field data but shows that  $\Delta \neq 0$  at temperatures as high as 4.5 mK. The recent noise-thermometer measurements of  $\Delta(T)$  are at least qualitatively consistent with the critical field data.

REFERENCES

- \* Work supported by the U. S. Atomic Energy Commission.
  - † Present address: Department of Physics, Stanford University  
Stanford, California 94305.
  - ‡ Present address: Royal Radar Establishment, Malvern,  
Worcestershire, U. K.
  - ‡ Present address: I. Physics Institute  
Free University of Berlin  
20 Boltzmannstrasse, 1 Berlin 33, Germany
1. J. W. Gibson and R. A. Hein, Phys. Rev. Letters 12, 688 (1964).
  2. R. T. Johnson, O. E. Vilches, J. C. Wheatley, and S. Gygax,  
Phys. Rev. Letters 16, 101 (1966).
  3. W. C. Black, Phys. Res. Letters 21, 597 (1966).
  4. W. C. Black, R. T. Johnson, and J. C. Wheatley, J. Low Temp.  
Phys. 1, 641 (1969).
  5. This work has been reviewed recently by John C. Wheatley, in  
Progress in Low Temperature Physics, Vol. VI, C. J. Gorter, Ed.,  
North Holland Publishing Company, Amsterdam, 1970, p. 77.
  6. J. Bardeen, L. N. Copper and J. R. Schrieffer, Phys. Rev. 108,  
1175 (1957).
  7. J. P. Maita, quoted by T. H. Geballe, Rev. Mod. Phys. 36, 134  
(1964).

8. E. Bucher, F. Heiniger, and J. Müller, Proceedings of the Ninth International Conference on Low Temperature Physics, Columbus, Ohio, 1964, J. G. Daunt, D. O. Edwards, F. J. Milford, and M. Yaquib, eds., Plenum Press, New York, 1965, p. 1059.
9. B. M. Abraham and Y. Eckstein, Phys. Rev. Letters 20, 649 (1968); 24, 663 (1970).
10. T. L. Thorp, et al., J. Low Temp. Phys. 3, 589 (1970).
11. Semi-Elements Inc., Saxonburg Blvd., Saxonburg, Pennsylvania.
12. K. H. Berthel, Phys. Stat. Sol. 5, 159 (1964).
13. F. G. Brickwedde, H. van Dijk, M. Durieux, J. R. Clement, and J. K. Logan, J. Res. Natl. Bur. Std. (U.S.) 64A, 1 (1960).
14. Temperatures on this scale are 10 mK lower than on the one described by H. J. Hoge and F. G. Brickwedde, J. Res. Natl. Bur. Std. (U.S.) 22, 351 (1939).
15. Harmon Plumb and George Cataland, Metrologia 2, 127 (1966).
16. B. B. Triplett, Ph.D. thesis, University of California at Berkeley, 1970, unpublished: B. B. Triplett and Norman E. Phillips, Phys. Rev. Letters 27, 1001 (1971), and to be published.
17. D. W. Osborne, H. E. Flotow, and F. Schreiner, Rev. Sci. Instr. 38, 159 (1967).
18. A compilation of recent measurements is given by Norman E. Phillips, Critical Reviews in Solid State Sciences 2, 467 (1971).
19. T. C. Cetas, C. R. Tilford, and C. A. Swenson, Phys. Rev. 174, 385 (1968).

20. A. J. Leadbetter and K. E. Wycherley, *J. Chem. Thermodynamics* 2, 855 (1970).
21. T. R. Waite, R. S. Craig, and W. E. Wallace, *Phys. Rev.* 104, 1240 (1956).
22. J. R. Clem, *Ann. Phys. (N.Y.)* 40, 268 (1966).
23. B. Mühlischlegel, *Z. Physik* 155, 313 (1959).
24. W. Parrish, *Acta Cryst.* 13, 838 (1960).
25. R. J. Corrucini and J. J. Gniewek, NBS Monograph 29, U. S. Government Printing Office, Washington, 1961.
26. E. A. Lynton, B. Serin, and M. Zucker, *J. Phys. Chem. Solids* 3, 165 (1957); G. Chanin, E. A. Lynton, and B. Serin, *Phys. Rev.* 114, 719 (1959).
27. P. W. Anderson, *J. Phys. Chem. Solids* 11, 26 (1959).
28. David Markowitz and Leo P. Kadanoff, *Phys. Rev.* 131, 563 (1963).
29. This estimate was based on the quantitative theory developed in ref. 28, values of normal-state parameters reported by E. Fawcett and D. Griffiths, *J. Phys. Chem. Solids* 23, 1631 (1962), and the resistivity ratios of the samples.
30. See, for example, G. Boato, G. Gallinaro, and C. Rizzuto, *Phys. Rev.* 148 353 (1966) and references therein; Klaus Schwidtal, *Z. Physik* 158, 563 (1960).
31. W. R. Decker and D. K. Finnemore, *Phys. Rev.* 172, 430 (1968).
32. S. Skalski, O. Betbeder-Matibet, and P. R. Weiss, *Phys. Rev.* 136, A1500 (1964).

33. A. A. Abrikosov and L. P. Gor'kov, Zh. Eksperim. i Teor. Fiz. 39, 178 (1960) [English transl.: Soviet Physics-JETP 12, 1243 (1961)].
34. W. L. McMillan, Phys. Rev. 167, 351 (1968).
35. L. F. Mattheiss, Phys. Rev. 139, A1893 (1965).
36. T. L. Loucks, Phys. Rev. 139, A1181 (1965).
37. T. L. Loucks, Phys. Rev. 143, 506 (1966).
38. F. H. Featherston and J. R. Neighbours, Phys. Rev. 130, 1324 (1963).
39. R. A. Webb, R. P. Giffard, and J. C. Wheatley, Phys. Letters 41A, 1 (1972).

Table I. Properties of tungsten samples.

| Measurement               | Measured Resistivity Ratio | Intrinsic Resistivity Ratio <sup>b</sup> | Physical Form of Sample              |
|---------------------------|----------------------------|--|--------------------------------------|
| BJW, critical field       | 7,500                      |  | $\frac{1}{8}$ " diam. single crystal |
| This work, heat capacity  | 57,000 <sup>a</sup>        | 67,000                                   | $\frac{1}{4}$ " diam. polycrystal    |
| This work, critical field | 17,000                     | 19,500                                   | $\frac{1}{8}$ " diam. polycrystal    |

<sup>a</sup> This value is the average of potentiometric and eddy current measurements on different sections of the rod. The two values differed by 20%.

<sup>b</sup> Calculated from the measured ratio from the data in Ref. 12.

Table II. Coefficients in Eq.(4) obtained by least-squares fits.

| Exponents of<br>included<br>terms | rms<br>deviation<br>(%) | $\gamma$<br>(mJ/mole K <sup>2</sup> ) | $A_3$<br>(mJ/mole K <sup>4</sup> ) | $A_5$<br>(mJ/mole K <sup>6</sup> ) | $A_7$<br>(mJ/mole K <sup>8</sup> ) | $A_9$<br>(mJ/mole K <sup>10</sup> ) | $A_{11}$<br>(mJ/mole K <sup>12</sup> ) |
|-----------------------------------|-------------------------|---------------------------------------|------------------------------------|------------------------------------|------------------------------------|-------------------------------------|--|
| 1,3,7                             | 0.51                    | 1.009                                 | $3.46 \times 10^{-2}$              |                                    | $2.66 \times 10^{-8}$              |                                     |  |
| 1,3,5,7                           | 0.50                    | 1.009                                 | $3.48 \times 10^{-2}$              | $-2.14 \times 10^{-5}$             | $3.05 \times 10^{-8}$              |                                     |  |
| 1,3,7,9                           | 0.51                    | 1.009                                 | $3.46 \times 10^{-2}$              |                                    | $2.56 \times 10^{-8}$              | $1.88 \times 10^{-12}$              |  |
| 1,3,5,7,9                         | 0.47                    | 1.008                                 | $3.51 \times 10^{-2}$              | $-1.01 \times 10^{-5}$             | $7.07 \times 10^{-8}$              | $-5.14 \times 10^{-11}$             |  |
| 1,3,7,9,11                        | 0.45                    | 1.009                                 | $3.48 \times 10^{-2}$              |                                    | $-1.78 \times 10^{-8}$             | $2.11 \times 10^{-11}$              | $-2.45 \times 10^{-13}$                |
| 1,3,5,7,9,11                      | 0.45                    | 1.008                                 | $3.48 \times 10^{-2}$              | $-4.58 \times 10^{-7}$             | $-1.42 \times 10^{-8}$             | $2.01 \times 10^{-10}$              | $-2.36 \times 10^{-13}$                |



Figure Captions

- Fig. 1 The sample holder-thermometer-heater assembly. The distance between the sample mounting thread and the thermometer is approximately 22 cm.
- Fig. 2 The heat capacity of tungsten as  $C/T$  vs.  $T^2$  for  $T < 4$  K. The straight line represents a graphical fit to the data in this temperature region.
- Fig. 3 The lattice heat capacity of tungsten as  $C_L/T^3$  vs.  $T^4$  for  $T > 4$  K. The straight line represents a graphical fit to the data in this temperature region.
- Fig. 4 The critical field of tungsten as  $H_C$  vs.  $T^2$ . The curves represent BCS theory fitted to the data as described in the text.
- Fig. 5 The critical field of tungsten as  $H_C^2$  vs.  $T^2$ , for  $T < 9$  mK. The solid curves represent BCS theory fitted to the data as described in the text. The dashed lines represent the limiting slope required by Eq.(2) with  $\gamma = 1.008$  mJ/mole  $K^2$ .
- Fig. 6 The critical field of tungsten plotted as deviations of the reduced critical field from parabolic temperature dependence vs. the square of the reduced temperature. In (a) the values of  $H_0$  were obtained by fitting to the BCS theory. In (b) the

values of  $H_0$  were obtained by extrapolating to 0 K according to Eq.(2) with  $\gamma = 1.008$  mJ/mole  $K^2$  (i.e. as shown by the dashed line in Fig. 6). The solid curves represent BCS theory and the dashed curves AG theory.

Fig. 7 The lattice heat capacity of tungsten plotted as  $\Theta$  vs.  $T$ . The solid square represents  $\Theta_0$  as calculated from elastic constants. The curve represents the temperature dependence of  $\Theta$  corresponding to  $A_3 = 3.46 \times 10^{-2}$  mJ/mole  $K^4$ ,  $A_7 = 2.84 \times 10^{-8}$  mJ/mole  $K^8$ , and all other coefficients in  $C_L$  equal to zero.

Fig. 8 Critical field of tungsten as determined by BJW, plotted as  $H_C^2$  vs.  $(T^* + \Delta)^2$  for various  $\Delta(T)$ . The straight lines correspond to Eq.(2) and  $\gamma = 1.008$  mJ/mole  $K^2$ .

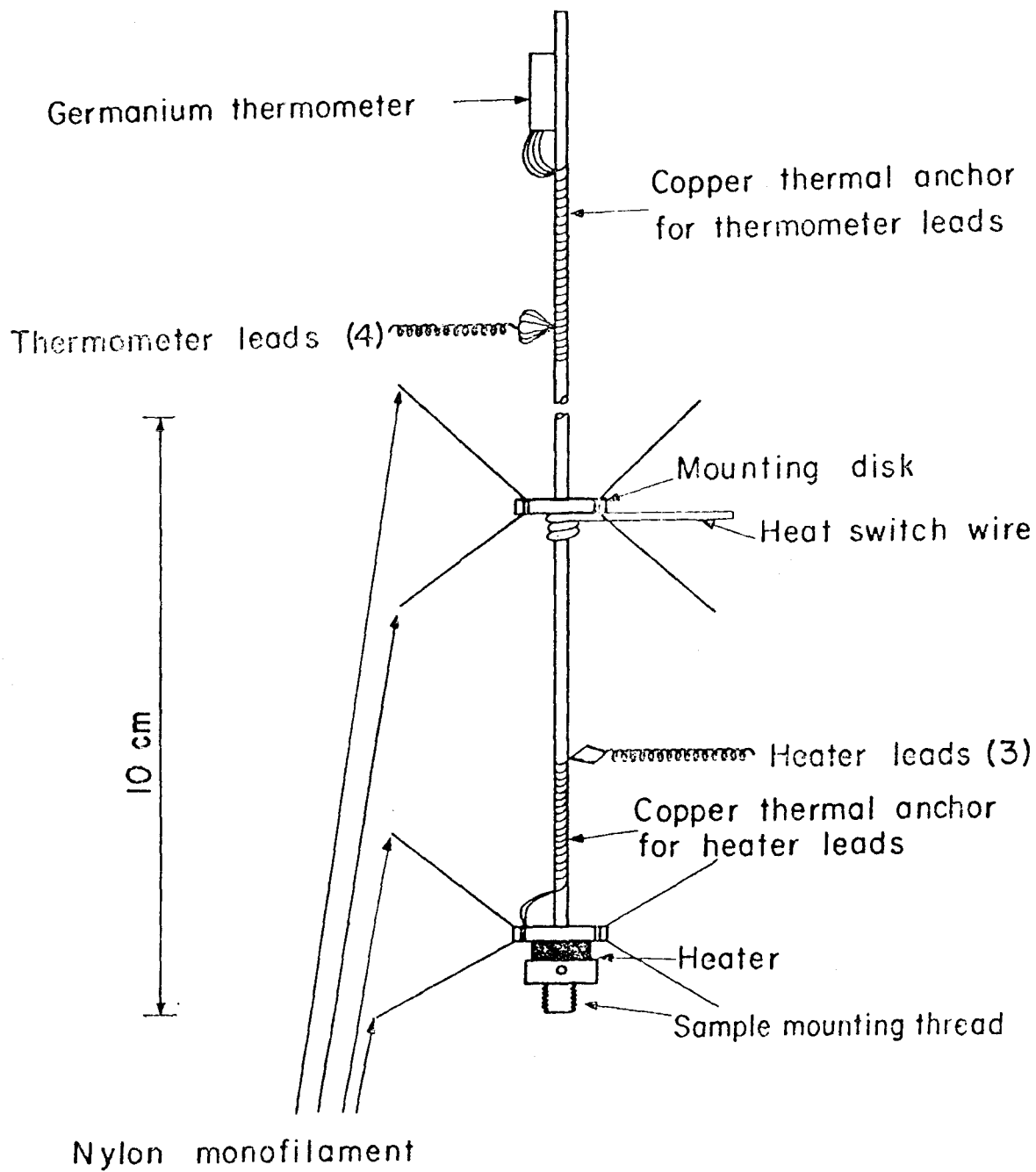
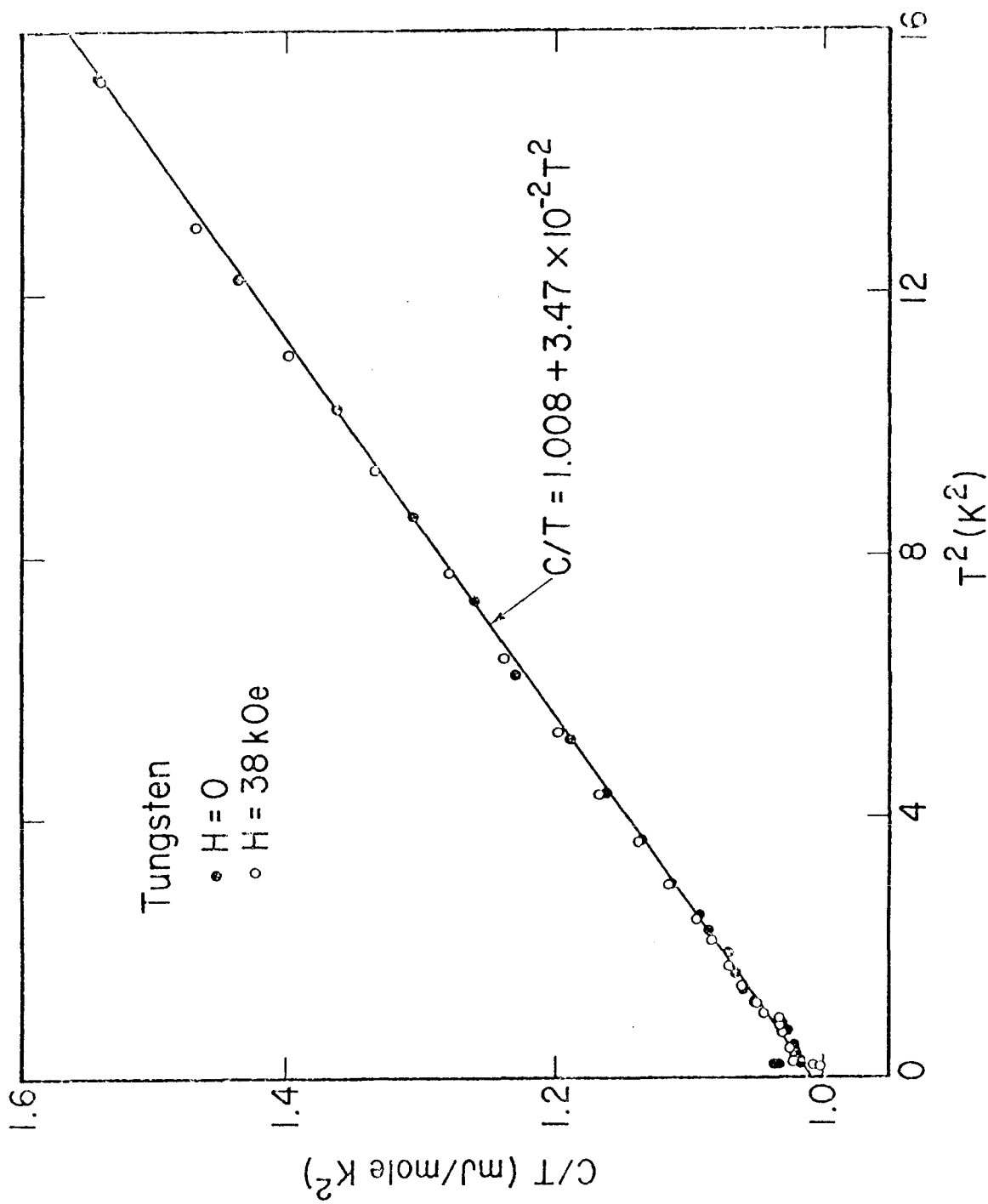
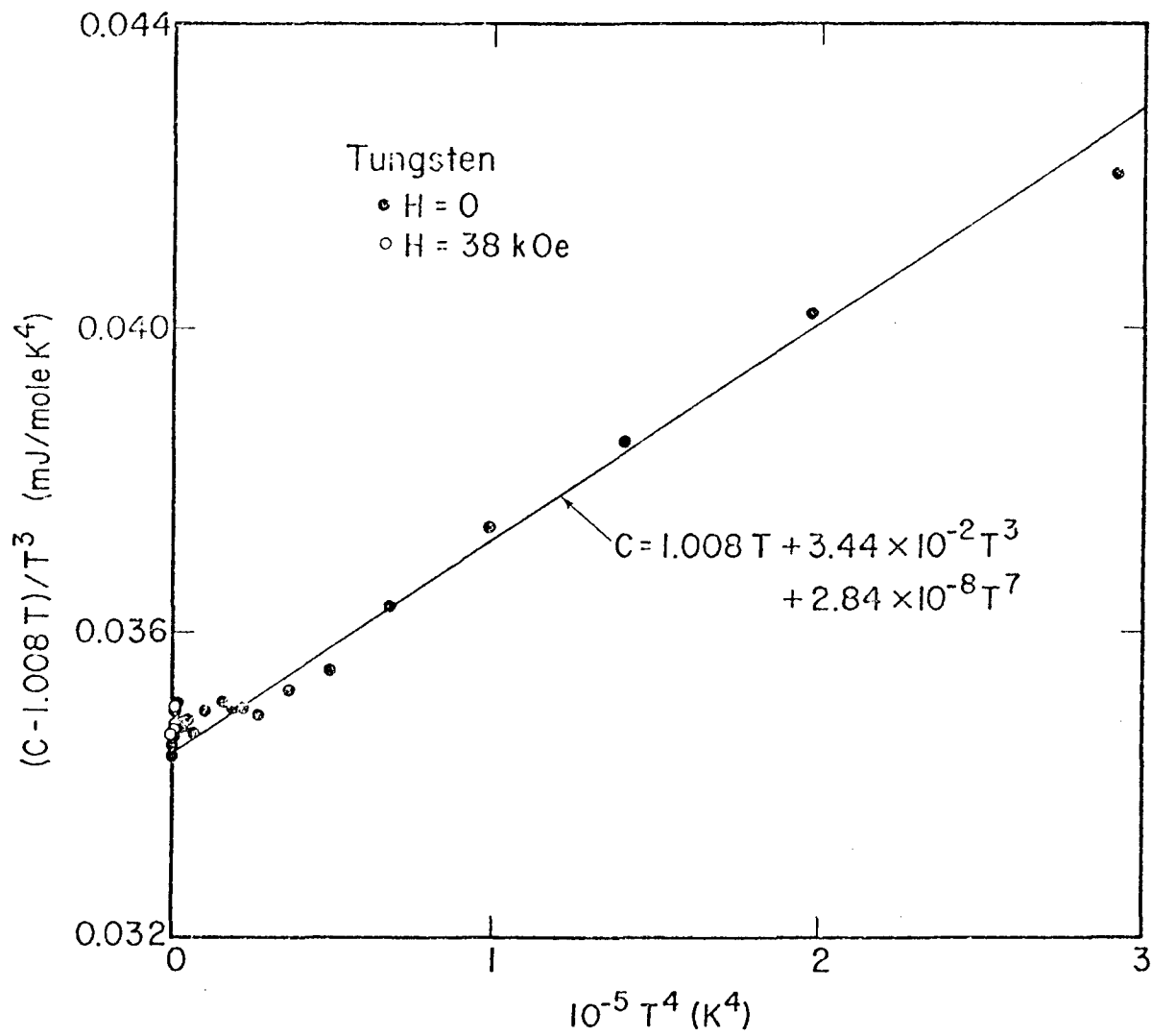


Figure 1



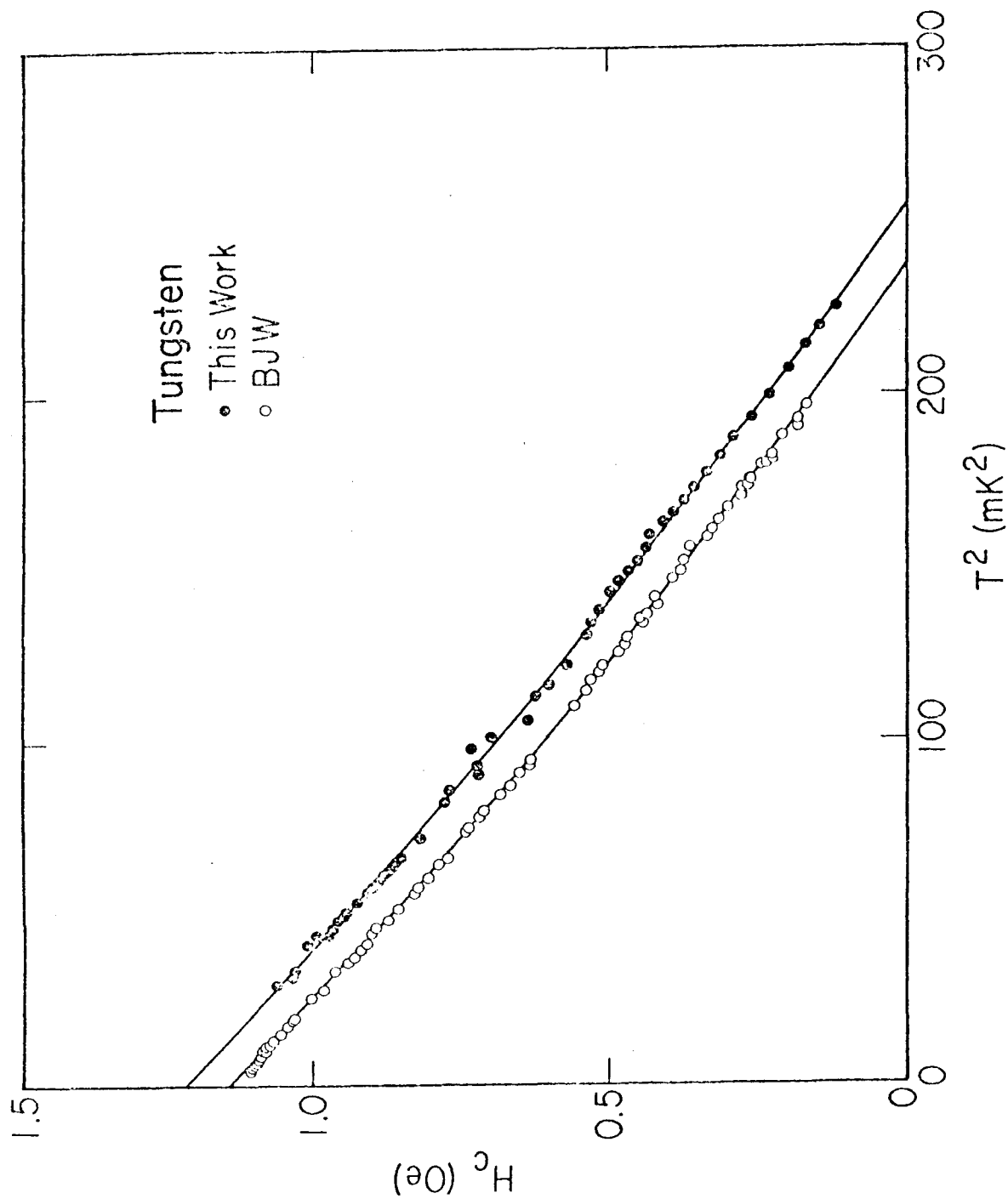
XBL 731-36

Figure 2



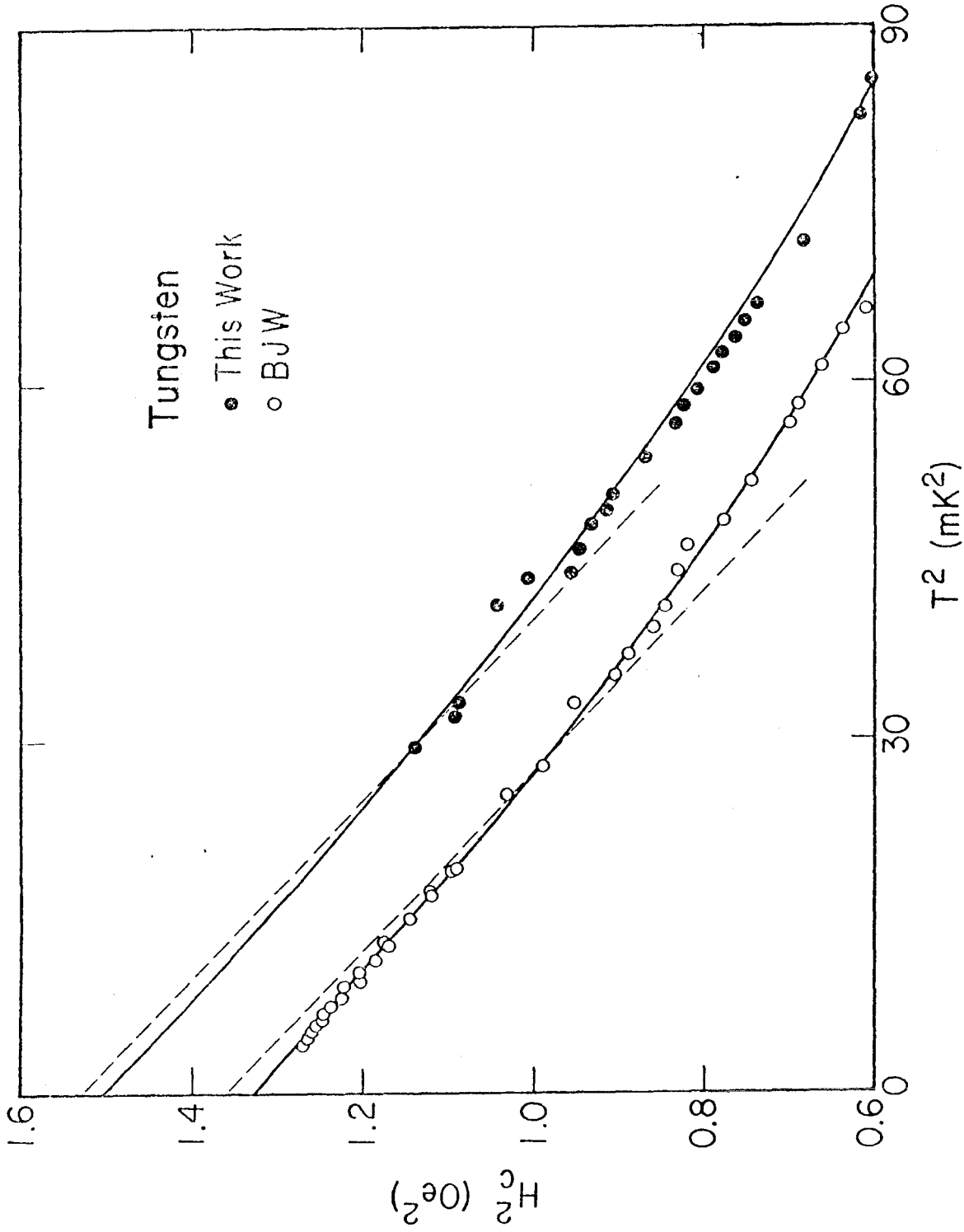
XBL 731-38

Figure 3



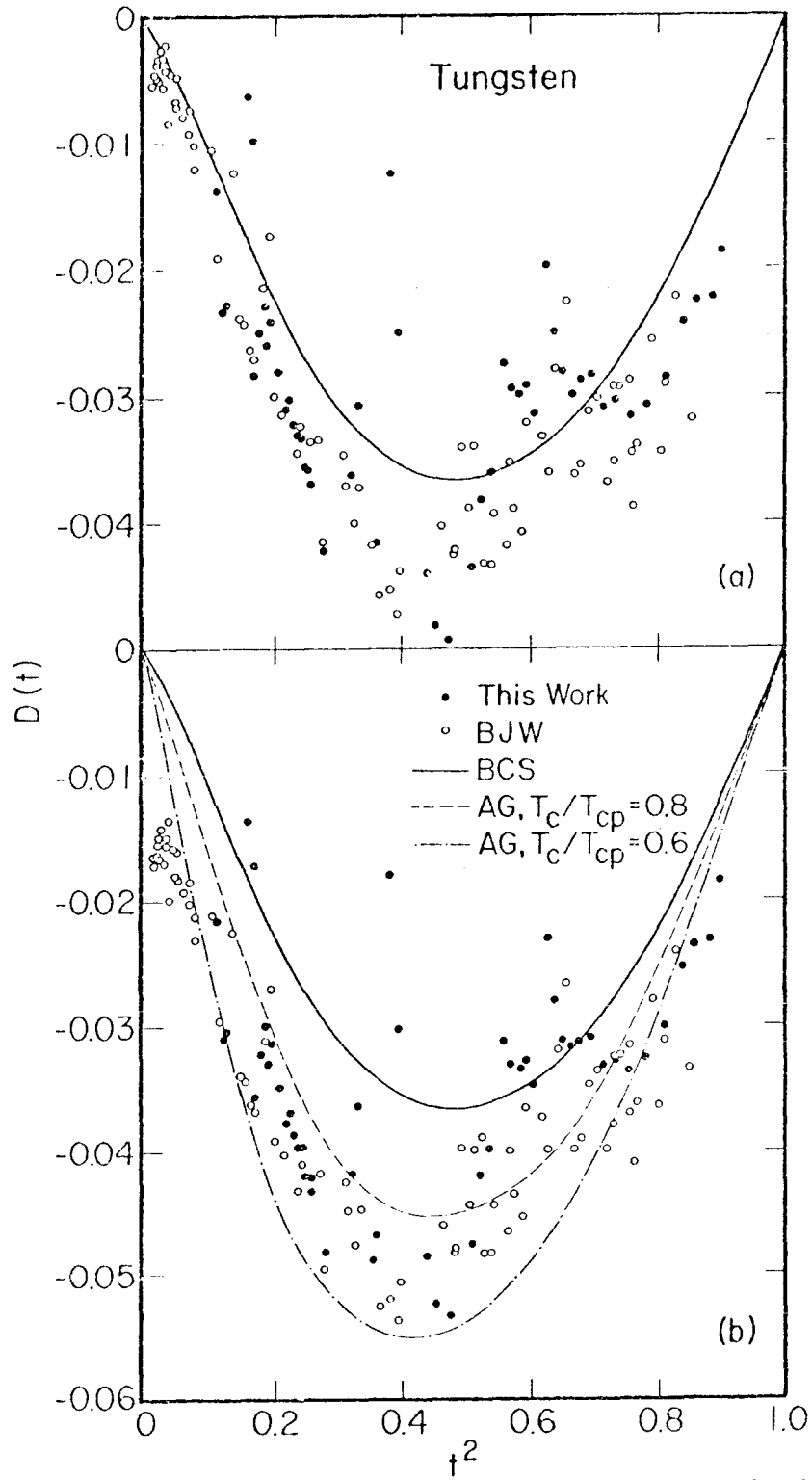
XBL 731-37

Figure 4

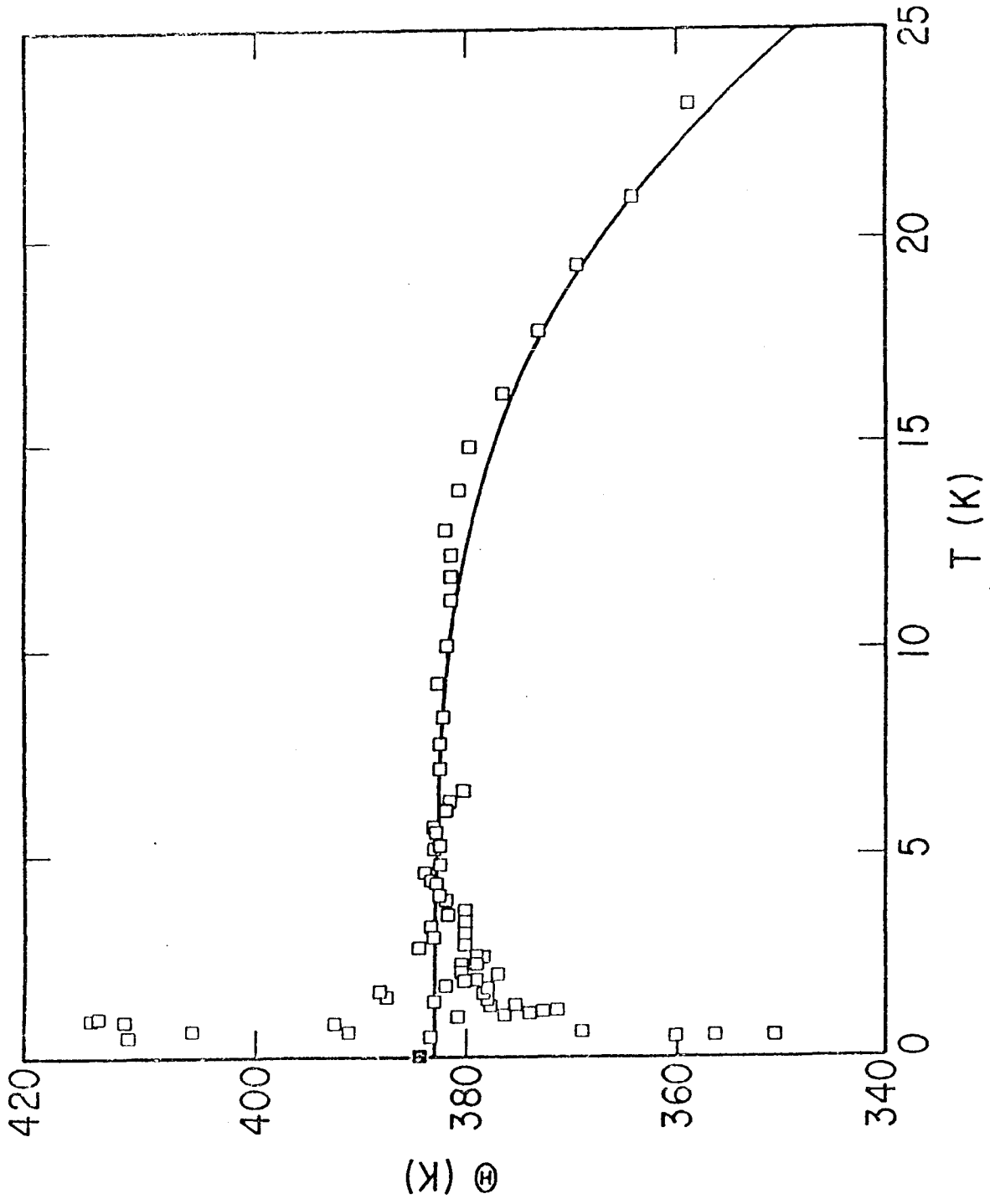


XBL 731-39

Figure 5

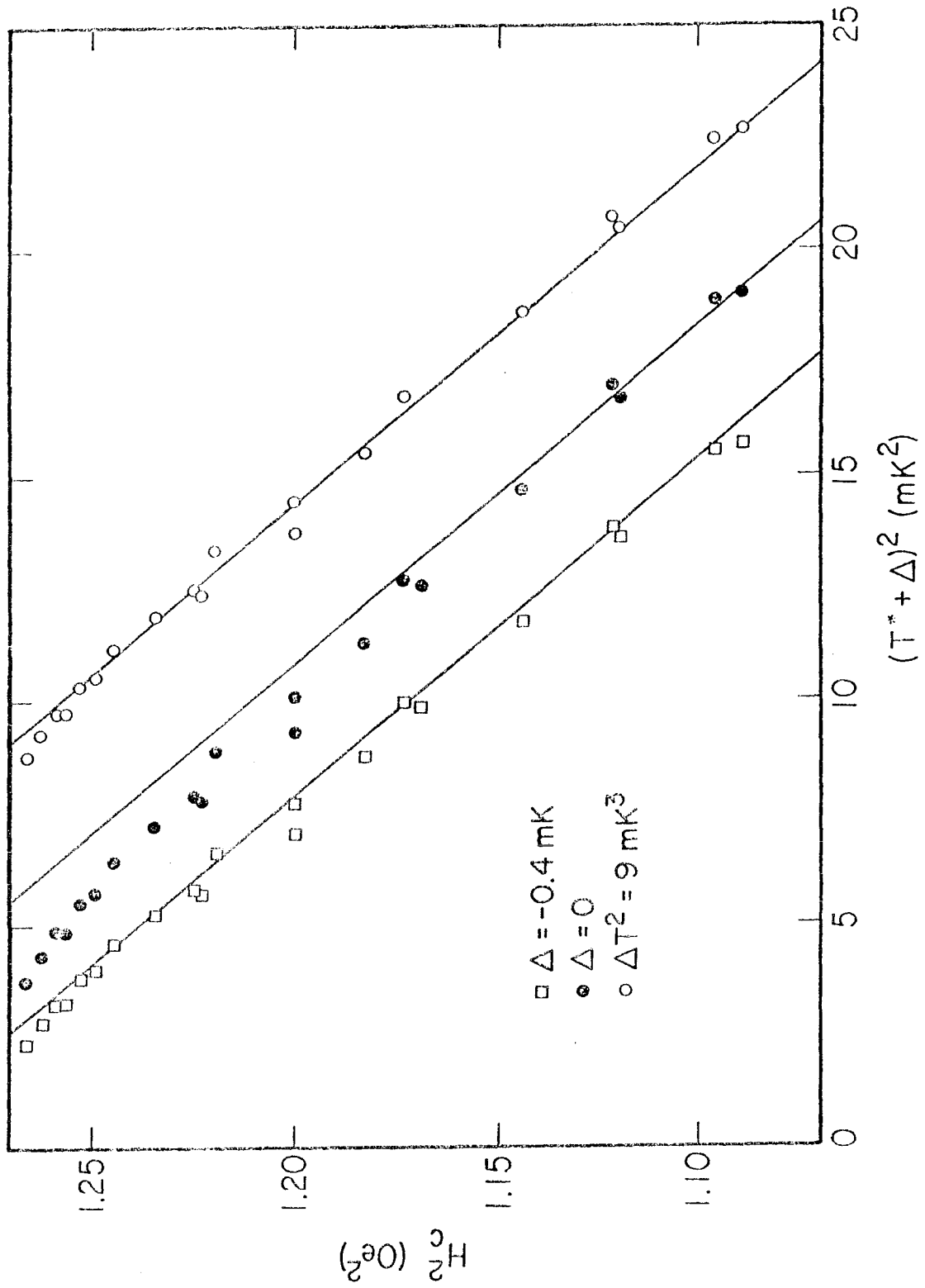






XBL 731-41

Figure 7



XBL 731-40

Figure 8